Deformable Reconstruction of Histology Sections Using Structural Probability Maps

Markus Müller[1], Mehmet Yigitsoy[1], Hauke Heibel[3], and Nassir Navab[1,2]

[1] Computer Aided Medical Procedures, Technische Universität München, Germany
[2] Computer Aided Medical Procedures, Johns Hopkins University, USA
[3] microDimensions GmbH, München, Germany

Abstract. The reconstruction of a 3D volume from a stack of 2D histology slices is still a challenging problem especially if no external references are available. Without a reference, standard registration approaches tend to align structures that should not be perfectly aligned. In this work we introduce a deformable, reference-free reconstruction method that uses an internal structural probability map (SPM) to regularize a free-form deformation. The SPM gives an estimate of the original 3D structure of the sample from the misaligned and possibly corrupted 2D slices. We present a consecutive as well as a simultaneous reconstruction approach that incorporates this estimate in a deformable registration framework. Experiments on synthetic and mouse brain datasets indicate that our method produces similar results compared to reference-based techniques on synthetic datasets. Moreover, it improves the smoothness of the reconstruction compared to standard registration techniques on real data.

1 Introduction

With a high resolution up to 0.25 µm, microscopy histology is an important technique to study anatomy on cellular level. Histology slices are created by cutting a tissue sample into ultra thin slices. These slices are then stained with certain chemicals in order to highlight different structures and finally the results are observed under a microscope. This process, however, introduces structural inconsistencies between slices: especially the stress put on the sample during cutting leads to deformations and artifacts such as holes, tears or foldings. Such artifacts make the reconstructing of a 3D volume from the individual slices very challenging. Nevertheless, such a reconstruction is very useful when assessing the progression of structures over several slices or creating atlases on micron level.

There are various techniques for reconstructing a histology volume. While global rigid/affine approaches are not able to correct for the local deformations resulting from the cutting procedure [1,2], a common approach applies several rigid/affine transformations on successive smaller subdivision of each image [3]. While this approach produces good results with a reasonable runtime, a local deformable registration is more suited to model the deformation of the cutting precedure and therefore improve the consistency between consecutive pairs. On the other hand this will also perfectly align structures that are not supposed to be

P. Golland et al. (Eds.): MICCAI 2014, Part I, LNCS 8673, pp. 122–129, 2014.

aligned anatomically, therefore straightening all features in stack direction and deviating from the original shape of underlying structures. Literally speaking, a deformable registration of a stack forming a cone would turn it into a cylinder which is not desirable.

One common approach to avoid this drift problem is to register each slice to an external reference. Either 3D in-vivo images such as Magnetic Resonance Images (MRI) [4] or so called block-face images, acquired by taking an image of the tissue block-face before cutting each histology slice [5], can be used as external references. While these methods provide excellent results, a reference is often not available. To circumvent the need for external references, Gaffling et al. [6] introduced a reference-free method that uses the regression of manually extracted landmarks to restrict the deformation. By using a polynomial regression over corresponding landmark positions, they obtain a smooth and consistent reconstruction of histology slices. Although the results of this method seem promising, given the large size of histology slices, manual extraction of landmarks is not feasible in practice and the author does not reference any method for automatic detection. Another reference-free method was proposed in [7] which extracts vessel structures from each slice and performs a rigid- followed by a deformable registration, that are both based on the extracted features. While this seems to produce very promising results on a liver sample, it is difficult to extend to samples that do not contain washed out vessel structures, like brain datasets.

In this paper, we propose two new, reference-free methods for 3D histology reconstruction that use the structural coherency of the histology data as an internal regularization. Our methods do not require any landmark extraction or blockface image acquisition processes. Inspired by [8], we employ the tensor voting framework [9] to extract a structural probability map (SPM), which contains a rough estimate of the original structures of the stack that should be retained by the registration. For structures that were destroyed in one slice, SPM can still be estimated from the surrounding slices. Coupled with the intensity similarity and the deformation regularization, SPM is used as a structural regularization constraint in the registration framework.

2 Methods

2.1 Structural Probability Map

Tensor voting is a conceptual grouping method that is employed for the inference of salient structures from a set of incoherent input points [9]. Inference is based on a communication scheme where every point, *voter*, casts its information that is encoded as a second order symmetric tensor, $\mathbf{T}$, to other sites, *votee*, over a hypothesized smooth curve with low total curvature. The strength of the vote cast depends on the voter's perceptual salience, the voter-to-votee distance, as well as the curvature of presumed curve connecting them. A votee at $\mathbf{y}$ accumulates incoming votes from all voters $\mathbf{x}$, using tensor addition $\mathbf{T}(\mathbf{y}) = \sum_{\mathbf{x}\in\mathcal{P}} \mathbf{A}^{\mathbf{x}}(\mathbf{y})$ where $\mathcal{P}$ is the set of voters and $\mathbf{A}^{\mathbf{x}}(\mathbf{y})$ is a tensor vote that $\mathbf{x}$ casts at $\mathbf{y}$. A tensor is represented as $\mathbf{T} = \sum_{d=1}^{\mathcal{D}} \lambda_d \hat{e}_d \hat{e}_d^T$ which can be decomposed as

$$\mathbf{T} = \sum_{d=1}^{\mathcal{D}-1}(\lambda_d - \lambda_{d+1})\sum_{k=1}^{d}\hat{e}_k\hat{e}_k^T + \lambda_{\mathcal{D}}\sum_{k=1}^{\mathcal{D}}\hat{e}_k\hat{e}_k^T \tag{1}$$
$$= \sum_{d=1}^{\mathcal{D}} s_d\mathcal{N}_d \quad \text{with} \quad s_d = \begin{cases}\lambda_d - \lambda_{d+1} & , d < \mathcal{D} \\ \lambda_{\mathcal{D}} & , d = \mathcal{D}\end{cases} \quad \text{and} \quad \mathcal{N}_d = \sum_{k=1}^{d}\hat{e}_k\hat{e}_k^T$$

where $\lambda_1 \geq \ldots \geq \lambda_{\mathcal{D}} \geq 0$ are eigenvalues, $\hat{e}_1 \ldots \hat{e}_{\mathcal{D}}$ are eigenvectors of $\mathbf{T}$, s_d is the salience, $\mathcal{N}_d$ is the d-D normal space, and $\mathcal{D}$ is the dimensionality of the space [10]. Every structure type is identified by the dimensionality, d, of its normal space, $\mathcal{N}_d$ and its strength is determined by the magnitude of its salience, s_d. Similar to the above decomposition, a tensor vote $\mathbf{A}^{\mathbf{x}}(\mathbf{y})$ can be written as

$$\mathbf{A}^{\mathbf{x}}(\mathbf{y}) = \sum_{d=1}^{\mathcal{D}} s_d^{\mathbf{x}}\mathbf{A}_d^{\mathbf{x}}(\mathbf{y}) \quad \text{with} \quad \mathbf{A}_d^{\mathbf{x}}(\mathbf{y}) = \sum_{j=1}^{d}\mathbf{S}_{d,j}^{\mathbf{x}}(\mathbf{y}) \tag{2}$$

where $\mathbf{A}_d^{\mathbf{x}}(\mathbf{y})$ is a vote for structure type d that consists of stick votes, $\mathbf{S}_{d,j}^{\mathbf{x}}(\mathbf{y})$, for each basis vector of $\mathcal{N}_d^{\mathbf{x}}$. Due to the limited space, we refer the reader to [9,8] for the details regarding the stick vote and communication scheme.

Let $I = (I_1, ..., I_n)$ be a stack of 2D images. We consider this stack as a volumetric image. We further define structural probability map images $SPM = (SPM_1, ..., SPM_n)$ where $SPM_i(\mathbf{y})$ is the structural saliency at $\mathbf{y}$. In this paper, we consider strong edges in images I_i detected by a standard 2D edge detector as the set of voters $\mathcal{P} = (\mathcal{P}_1, ..., \mathcal{P}_n)$ and every point in the SPM as votees. Inference is done by performing a voting for each votee and then extracting surface saliences from the accumulated tensors $\mathbf{T}(\mathbf{y})$ using Eq.1, which are set as scalar values for $SPM(\mathbf{y})$.

2.2 Consecutive Registration

We assume that the histology stack was already roughly pre-aligned by a standard rigid registration, thus our method aims to improve the smoothness by performing a modified deformable registration based on 2D Free-Form Deformations (FFDs). We model the deformations as a discrete optimization problem using Markov Random Fields (MRFs) [11]. A 2D FFD grid G^i is assigned to every slice I_i, thus each control point $\mathbf{p}$ resembles a node in the MRF. In order to model the actual displacement of control points we designate a labeling l of discrete values to all nodes. Each label $l_{\mathbf{p}}$ therefore describes the displacement $\mathbf{d}_{l_{\mathbf{p}}}$ of the control point $\mathbf{p}$ (see Fig. 1). The labeling problem can then be solved with a quadratic pseudo-boolean optimization (QPBO) algorithm [12].

In our first approach the labeling is solved consecutively for each slice I_i in the stack:

$$E_i(l) = \sum_{\mathbf{p}\in G^i}\Big(E_{data}(I_i, I_{i+1}, l_{\mathbf{p}}) + \gamma E_{SPM}(\mathcal{P}_i, SPM_i, l_{\mathbf{p}}) + \rho R(\mathbf{d}_{l_{\mathbf{p}}})\Big) \tag{3}$$

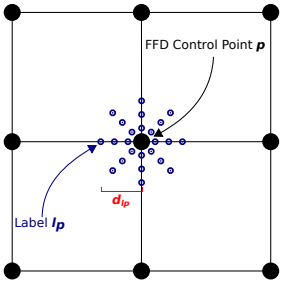

Fig. 1. Example for MRF labeling around a control point

γ and ρ weight the contribution of the regularization. E_{data} compares the deformed slice with the undeformed neighbour with a Normalized Cross Correlation (NCC), that yields robust results with lower computational cost. Other similarity measures like Mutual Information are possible but have not been tested yet.

$$E_{data}(I_i, I_{i+1}, l_{\mathbf{p}}) = \sum_{\mathbf{x}} NCC(I_i(\mathbf{x} + \mathbf{d}_{l_{\mathbf{p}}}), I_{i+1}) \tag{4}$$

We are not registering to the deformed neighbouring slice because this would accumulate deformations and therefore introduce a strong drift. Therefore this term alone can only align the slices roughly, because the deformations of two neighboring slices are not connected. However, the smoothness is improved by E_{SPM} that aligns the edges with the estimated structure map. Since the SPM represents the 3D structure of the stack, it also contrains the 2D FFDs in order to respect the global consistency of the structures and avoid clustering.

$$E_{SPM}(\mathcal{P}_i, SPM_i, l_{\mathbf{p}}) = \sum_{\mathbf{x}} NCC(\mathcal{P}_i(\mathbf{x} + \mathbf{d}_{l_{\mathbf{p}}}), SPM_i) \tag{5}$$

The energy R penalizes implausible or unnatural deformations and, in our case, depends only on the distance of all in-plane neighbours $N(\mathbf{p})$ of each control point $\mathbf{p}$:

$$R(l_{\mathbf{p}}) = \sum_{r \in N(\mathbf{p})} ||\mathbf{d}_{l_{\mathbf{p}}} - \mathbf{d}_{l_r}||^2 \tag{6}$$

The consecutive registration method has the advantage of being fast and performs well when the stack does not involve too complex structures or deformations (e.g. the synthetic data used in section 3.1). However, because the deformations are not directly connected between slices, its performance deteriorates when the tissue deformations are complicated which is often the case in real histology data.

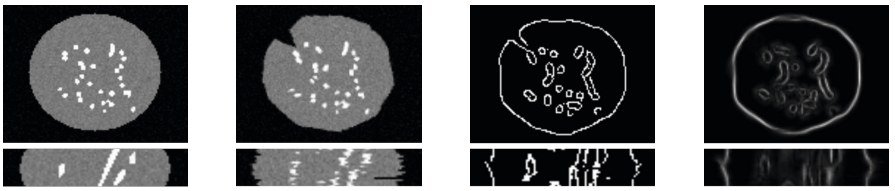

(a) (b) (c) (d)

Fig. 2. Synthetic dataset: (a) undeformed stack, (b) corrupted stack, (c) edge map, (d) structural probability map

2.3 Simultaneous Registration

Therefore, we extended our algorithm to register the whole stack simultaneously, which is computational more expensive but also produces better results. For this we employ a method similar to the one proposed in [5], which splits the MRF energy into one pair-wise term and two unary ones.

$$E(l) = \sum_{i=1}^{n-1} \sum_{\substack{\mathbf{p}\in G^i \\ \mathbf{q}\in G^{i+1}}} E_{data}(I_i, I_{i+1}, l_\mathbf{p}, l_\mathbf{q}) + \sum_{i=1}^{n} \sum_{\mathbf{p}\in G^i} \Big(\gamma E_{SPM}(\mathcal{P}_i, SPM_i, l_\mathbf{p}) + \rho R(l_\mathbf{p})\Big) \tag{7}$$

In this formulation, the unary terms E_{SPM} and R stay the same as Eqs. 5 and 6 respectively and act as in-plane regularizations. However, to make the model better, we recapitulate the data term E_{data} in a pair-wise manner by coupling the deformations of neighboring slices.

$$E_{data}(I_i, I_{i+1}, l_\mathbf{p}, l_\mathbf{q}) = \sum_{\mathbf{x}} NCC(I_i(\mathbf{x} + \mathbf{d}_{l_\mathbf{p}}), I_{i+1}(\mathbf{x} + \mathbf{d}_{l_\mathbf{q}})) \tag{8}$$

Contrary to Eq. 4, the term now connects the control points (or more accurately its labels) of neighboring slices, thus significantly increasing their possible alignment. This also means that the weighting γ should be treated differently in the simultaneous case (Eq. 7) than in the consecutive one (Eq. 3), because E_{SPM} is now only responsible for the regularization and no more for the smoothness itself. For the consecutive one we empirically found out that $\gamma = 1.0$ is good overall value but can be increased if the structure map is of good quality. Whereas for the simultaneous registration, a lower value around 0.5 usually produces regularized but still structurally consistent results.

3 Experimental Validation and Results

3.1 Synthetic data

We performed experiments on synthetic and real data. The synthetic data consists of a stack of 20 slices with a resolution of 128x96 and a pixel spacing of

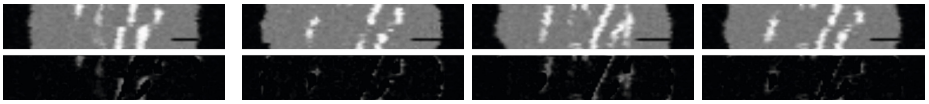

(a) (b) (c) (d)

Fig. 3. Reconstruction results in the first row and absolute difference with Fig. 2(a) in the second. (a) Consecutive Registration w/o SPM, (b) Consecutive Registration w/ SPM, (c) Simultaneous Registration w/o SPM, (d) Simultaneous Registration w/ SPM.

1mm. An example of an original slice is shown in Fig. 2(a). The slices contain a circular tissue which grows to the middle and several skewed vascular structures. Each slice is deformed by a random FFD with a maximum displacement of 5mm and the deformation field is saved as ground truth. Additional tears are introduced in randomly selected slices to simulate the real histology cutting process. Distorted slices are shown in Fig. 2(b).

In order to quantify the results of our method, we calculated the absolute end point error (EE) and the relative angular error (AE) between the resulting deformation fields and the ground truth fields [13]. Table 1 shows the errors after the application of different reconstruction approaches discussed here.

Table 1. End point error (EE) and angular error (AE) of the presented methods

Method	EE		AE	
	Error (mm)	STD (mm)	Error (°)	STD (°)
Consecutive Registration w/o SPM	2.91	1.78	60.31	31.41
Consecutive Registration w/ SPM	1.69	1.25	45.39	26.63
Simultaneous Registration w/o SPM	2.37	1.27	57.31	33.17
Simultaneous Registration w/ SPM	1.68	1.13	45.95	26.89

For the registration we used a grid spacing of 15mm and 2 grid levels. In the consecutive case both ρ and γ were set to 1.0 in order to put more emphasis on the structural map. For the simultaneous method, we used 0.5 for both instead. The results in Fig. 3 show the same coronal slice as Fig. 2.

The consecutive registration without the SPM regularization performs worst in terms of the error but also in it's visual appearance (c.f. Fig. 3(a)). All curvilinear structures get straightened in stack direction and especially two vessel structures on the right side cluster into four distinctive structures. Extending this with our SPM maintains the outer round shape but also preserves the curvilinearity of the vessels inside (Fig. 3(b)). This is similiar for the simultaneous method: while the unregularized registration (Fig. 3(c)) does perform significantly better than the unregularized consecutive method from a visual perspective, it still produces a high error which can be again compensated with the use of our SPM. Since the

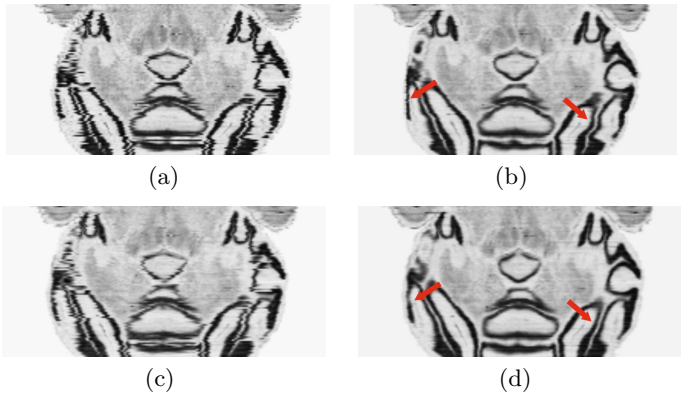

Fig. 4. Coronal view of the reconstructed mouse brain dataset: (a) rigidly aligned source stack, (b) simultaneous registration w/o SPM, (c) consecutive registration w/ SPM, (d) simultaneous registration w/ SPM.

simultaneous methods put more emphasis on aligning the actual image data, the reconstructed stacks have a slightly smoother appearance (Fig. 3(c)). However, without the regularization through a structure map, there is a drift error. Also the results of both of our methods are visually closer to the original stack in Fig. 2(a) than the unregularized methods.

3.2 Mouse Brain

We also performed experiments on a mouse brain dataset of 100 slices with 213x168 pixel that was provided online by [14]. Since the spacing was missing, we assumed it to be 1mm. The FFD grid size was therefore set to 20mm and subdivided on 3 grid levels. γ and ρ were set to 0.5 again. The slices were aligned rigidly before hand (see Fig. 4(a)). Since there is no ground truth available, only visual results are provided. As indicated before, the consecutive method (Fig. 4(c)) improves the stack consistency over the source stack but the result is less smooth than the unregularized simultaneous method (Fig. 4(b)). Our simultaneous method (Fig 4(d)), however, improves the results significantly over the other two approaches. It especially corrects drift errors that are present on the highlighted structures in Fig. 4(b). The overall simultaneous reconstruction including the tensor voting took around 20 minutes while the consecutive one only needs around 7 minutes which is a potential advantage on big datasets.

4 Discussion and Conclusion

In this work we presented a new, reference free method for histology stack alignment. We make use of tensor voting technique as a means to recover structural information that has been corrupted by the histology cutting process. Our experiments show that the proposed algorithm can improve upon conventional

method. However, our method can only maintain structures that are still present in the corrupted stack and is therefore not meant as a replacement for reference-based methods but in the case when no reference is available. Due to the FFD formulation, the proposed method is unable to correctly close tears, a problem that should be addressed in future work. In order to use the algorithm on full resolution histology stack, the implementation also requires a more sophisticated memory management and subdivision of the data both for the tensor voting and the registration itself. This project has been partially supported by SFB 824.

References

1. Malandain, G., Bardinet, E., Nelissen, K., Vanduffel, W.: Fusion of autoradiographs with an mr volume using 2-d and 3-d linear transformations. NeuroImage 23(1), 111–127 (2004)
2. Cifor, A., Bai, L., Pitiot, A.: Smoothness-guided 3-d reconstruction of 2-d histological images. NeuroImage 56(1), 197–211 (2011)
3. Likar, B., Pernuš, F.: Registration of serial transverse sections of muscle fibers. Cytometry 37(2), 93–106 (1999)
4. Bardinet, E., Ourselin, S., Dormont, D., Malandain, G., Tandé, D., Parain, K., Ayache, N., Yelnik, J.: Co-registration of histological, optical and mr data of the human brain. In: Dohi, T., Kikinis, R. (eds.) MICCAI 2002, Part I. LNCS, vol. 2488, pp. 548–555. Springer, Heidelberg (2002)
5. Feuerstein, M., Heibel, H., Gardiazabal, J., Navab, N., Groher, M.: Reconstruction of 3-d histology images by simultaneous deformable registration. In: Fichtinger, G., Martel, A., Peters, T. (eds.) MICCAI 2011, Part II. LNCS, vol. 6892, pp. 582–589. Springer, Heidelberg (2011)
6. Gaffling, S., Daum, V., Hornegger, J.: Landmark-constrained 3-D histological imaging: A morphology-preserving approach. In: VMV, pp. 309–316 (2011)
7. Schwier, M., Böhler, T., Hahn, H.K., Dahmen, U., Dirsch, O.: Registration of histological whole slide images guided by vessel structures. Journal of Pathology Informatics 4(suppl.) (2013)
8. Yigitsoy, M., Navab, N.: Structure propagation for image registration. IEEE Transactions on Medical Imaging 32(9), 1657–1670 (2013)
9. Medioni, G., Tang, C., Lee, M.: Tensor voting: Theory and applications. In: Proceedings of RFIA, Paris, France (2000)
10. King, B.: Range data analysis by free-space modeling and tensor voting. ProQuest (2008)
11. Glocker, B., Komodakis, N., Tziritas, G., Navab, N., Paragios, N.: Dense image registration through mrfs and efficient linear programming. Medical Image Analysis 12(6), 731–741 (2008)
12. Kolmogorov, V., Rother, C.: Minimizing nonsubmodular functions with graph cuts-a review. TPAMI 29(7), 1274–1279 (2007)
13. Baker, S., Scharstein, D., Lewis, J., Roth, S., Black, M.J., Szeliski, R.: A database and evaluation methodology for optical flow. IJCV 92(1), 1–31 (2011)
14. Ju, T., Warren, J., Carson, J., Bello, M., Kakadiaris, I., Chiu, W., Thaller, C., Eichele, G.: 3d volume reconstruction of a mouse brain from histological sections using warp filtering. Journal of Neuroscience Methods 156(1), 84–100 (2006)